

## Generalized $W$ state of four qubits with exclusively the three-tangle

Sebastian Gartzke and Andreas Osterloh\*

*Institut für Theoretische Physik, Universität Duisburg-Essen, D-47048 Duisburg, Germany*

 (Received 22 December 2017; revised manuscript received 10 July 2018; published 6 November 2018)

We single out a class of states possessing only the three-tangle but distributed all over four qubits. This is a three-site analog of states from the  $W$  class. The latter possess exclusively globally distributed pairwise entanglement as measured by the concurrence. We perform an analysis for four qubits, showing that such a state indeed exists. To this end we analyze specific states of four qubits for which all possible SL invariants vanish, and hence which are part of the SL null cone. Instead, they will possess a certain unitary invariant. In analyzing the three-tangle of rank-two reduced density matrices of these states, we manage to show that in this particular case we reach the convex roof exactly. As an interesting by-product this solution is extended in the rank-two case to a homogeneous polynomial SL-invariant measure of entanglement of degree  $2m$ , if there are two states which correspond to an at most  $n$ -fold degenerate solution in the zero polytope for  $0 < n < m$  that can be combined with the convexified minimal characteristic curve at an  $(2m - n)$ -fold zero yielding a decomposition of  $\rho$ . If more than one such state does exist in the zero polytope, a minimization must be performed. If no decomposition of  $\rho$  is obtained in this way, it provides a better lower bound than the lowest convexified curve.

DOI: [10.1103/PhysRevA.98.052307](https://doi.org/10.1103/PhysRevA.98.052307)

### I. INTRODUCTION

$W$  states are at the borderline of three distinct and important features of multipartite entanglement: pure  $W$  states satisfy the Coffman-Kundu-Wootters (CKW) inequality [1,2] as an equality [1], they are representatives of one of two possible classes of entanglement for three qubits [3], and they naturally emerge from a ladder that bridges SL invariance down to U invariance [4] for an arbitrary number of qubits. Indeed, three qubits are separated into the Greenberger-Horne-Zeilinger (GHZ) class which is detected by the three-tangle [1] and the remaining  $W$  class sharing entanglement among at most two parties [1]. A further peculiarity of the  $Q$ -qubit  $W$  state is hence that it has no SL-invariant  $n$ -tangle with  $n > 2$  [5,6].

It is therefore reasonable to ask the following question: do such states also exist for  $Q$  qubits and an arbitrary  $n < Q$ ; in other words, are there certain  $Q$ -qubit states possessing only an  $n$ -tangle? In particular the corresponding states should not possess any SL-invariant  $Q$ -tangle (that is, a  $(2m, 0)$  bidegree of unitary invariants on  $Q$  sites [7]) and thus should be part of the SL null cone. The SL null cone, however, has a finer structure which is classified further by SU invariants with the bidegree  $(2m - l, l)$  (see, e.g., Ref. [7]). SU invariants of bidegree  $(2m - l, l)$  are  $(2m - l)$  linear in the wave function  $\psi$  and are  $l$  linear in its complex conjugate  $\psi^*$  (or vice versa). Every state situated outside the null cone must always have a part which is balanced [6] or equivalently termed c-balanced (c for convex) in Ref. [4]. In contrast, there are those states which are a-balanced (a for affine) without having a c-balanced part. Those states are singled out by possessing discrete topological phases under the cyclic local SU group operation [8]. They emerge from the c-balanced states by

means of *partial spin flips* [4]. For three qubits simple examples are the states in the SL  $W$  class

$$|W_3(\vec{c})\rangle = c_0|000\rangle + c_1|100\rangle + c_2|010\rangle + c_3|001\rangle, \quad (1)$$

which do possess an SU invariant of bidegree  $(3,1)$ . These states, by means of a partial spin flip, are connected to the  $(4,0)$ -invariant states which are in the SL-invariant GHZ class

$$|\text{GHZ}_3(\vec{c})\rangle = c_0|111\rangle + c_1|100\rangle + c_2|010\rangle + c_3|001\rangle. \quad (2)$$

In both formulas  $\vec{c} = (c_0, c_1, c_2, c_3)$ , where in the states from the GHZ class  $c_i \neq 0$  for  $i = 0, \dots, 3$ . The original  $W$  states ( $c_0 = 0$ ) are however  $(q, q)$  invariant and are SL equivalent but not U equivalent to  $|W_3(c_0, c_1, c_2, c_3)\rangle$  with nonzero  $c_0$ . They do not emerge from this procedure after performing  $Q$  partial spin flips since they are completely unbalanced states [6]. They are, however, obtained when omitting some product basis state from the outcome of such a procedure. Nevertheless, every state displaying a unitary  $(2m - l, l)$  invariant and having no  $(2m, 0)$  invariant will be a good starting point to look at as soon as it is not a bipartite state.

This article is organized as follows. In the next section we describe the states we are analyzing. In Sec. III we emphasize details about the calculation of the convex roof of the three-tangle and focus on those states which contain only the three-tangle. In the conclusions we summarize the obtained results and give an outlook.

### II. STATES FROM THE SL NULL CONE

We start from the four-qubit maximally entangled c-balanced states:

$$|\Psi_6^A\rangle = \frac{1}{\sqrt{3}}|1111\rangle + \sqrt{\frac{2}{3}}|W^A\rangle, \quad (3)$$

$$|\Psi_4^A\rangle = \frac{1}{2}(|1111\rangle + |1100\rangle + |0010\rangle + |0001\rangle), \quad (4)$$

\*andreas.osterloh@uni-due.de

where  $|W^4\rangle = (|1000\rangle + |0100\rangle + |0010\rangle + |0001\rangle)/2$  is a completely unbalanced  $W$  state of four qubits. We define the extended length of a state as follows:

*Definition II.1 (extended length).* Let  $|\psi\rangle$  be a balanced state in its minimal representation of length  $L$  after local SU operations and let  $A_{|\psi\rangle}$  be its corresponding alternating matrix [6]. Following Ref. [6]

$$\exists n_1, \dots, n_L \in \mathbf{N} \quad (n_j > 0) \ni$$

$$\sum_{j=1}^L n_j (A_{|\psi\rangle})_{ij} = 0 \quad \forall i \in \{1, \dots, Q\}.$$

Then we define the *extended length* of the state as

$$L_{\text{ext}} = \sum_{i=1}^L n_i.$$

We want to highlight that the extended length has to be an even number. Here,  $|\Psi_{L_{\text{ext}}}^Q\rangle$  means a  $Q$  qubit state which is irreducibly c-balanced of extended length  $L_{\text{ext}} = 2n$ ,  $n \in \mathbf{N}$ .

### A. States derived from $\Psi_6^4$

The state taken from Eq. (3) is detected by the only genuine (6,0) filter invariant [4,6,9,10] of SU giving a nonzero result due to its extended length of  $L_{\text{ext}} = 6$ . Possible states in the SL null cone therefore have (5,1), (4,2), and (3,3) invariance [4] and are obtained by a partial spin flip on one, two, or three components, respectively, of the product basis. Since the state is translation symmetric (even with respect to the symmetric group of permutations) it does not matter which of the four components of the  $W^4$  state the partial spin flips are acting on. Therefore we have a single case of (5,1), (4,2), and (3,3) invariance each and one (4,2) invariant acting on the  $|1111\rangle$  component together with a (3,3) invariant if the next partial spin flip is acting on the  $W^4$  state. The (3,3)-invariant states, however, are bipartite product states and therefore are not considered any further. We are left with the following states:

$$|\Psi_{6;1}^4\rangle = \frac{1}{\sqrt{3}}|0000\rangle + \sqrt{\frac{2}{3}}|W^4\rangle, \quad (5)$$

$$|\Psi_{6;2}^4\rangle = \frac{1}{\sqrt{3}}|1111\rangle + \frac{1}{\sqrt{6}}(|0111\rangle + |0100\rangle + |0010\rangle + |0001\rangle), \quad (6)$$

$$|\Psi_{6;23}^4\rangle = \frac{1}{\sqrt{3}}|1111\rangle + \frac{1}{\sqrt{6}}(|0111\rangle + |1011\rangle + |0010\rangle + |0001\rangle), \quad (7)$$

where the indices after the semi-colon indicate where the partial spin flip operation acts on. For example, for  $|\Psi_{6;234}^4\rangle$  we would have it acting on the components 2, 3, and 4 of the state  $|\Psi_6^4\rangle$ .

The state  $|\Psi_{6;1}^4\rangle$  becomes a mixture of states in the  $W$  class—it therefore contains no three-tangle; states  $|\Psi_{6;2}^4\rangle$  and  $|\Psi_{6;23}^4\rangle$  may contain a three-tangle instead.

The three-tangle is given by [1] (see also Refs. [9,11,12])

$$\tau_3 = 4|d_1 - 2d_2 + 4d_3| \quad (8)$$

$$= \left| \sum_{\mu=0}^3 g_\mu (\sigma_\mu \otimes \sigma_y \otimes \sigma_y) \bullet (\sigma_\mu \otimes \sigma_y \otimes \sigma_y) \right|, \quad (9)$$

$$d_1 = \psi_{000}^2 \psi_{111}^2 + \psi_{001}^2 \psi_{110}^2 + \psi_{010}^2 \psi_{101}^2 + \psi_{100}^2 \psi_{011}^2, \quad (10)$$

$$d_2 = \psi_{000} \psi_{111} \psi_{011} \psi_{100} + \psi_{000} \psi_{111} \psi_{101} \psi_{010} + \psi_{000} \psi_{111} \psi_{110} \psi_{001} + \psi_{011} \psi_{100} \psi_{101} \psi_{010} + \psi_{011} \psi_{100} \psi_{110} \psi_{001} + \psi_{101} \psi_{010} \psi_{110} \psi_{001}, \quad (11)$$

$$d_3 = \psi_{000} \psi_{110} \psi_{101} \psi_{011} + \psi_{111} \psi_{001} \psi_{010} \psi_{100}, \quad (12)$$

with the Pauli matrices

$$\sigma_0 := \mathbb{1}_2 = \begin{pmatrix} 1 & 0 \\ 0 & 1 \end{pmatrix}, \quad \sigma_1 := \sigma_x = \begin{pmatrix} 0 & 1 \\ 1 & 0 \end{pmatrix},$$

$$\sigma_2 := \sigma_y = \begin{pmatrix} 0 & -i \\ i & 0 \end{pmatrix}, \quad \sigma_3 := \sigma_z = \begin{pmatrix} 1 & 0 \\ 0 & -1 \end{pmatrix},$$

and  $g_\mu = (-1, 1, 0, 1)$ , where the notation of Refs. [5,9] is used. In what follows we use the square root of the three-tangle to measure three-partite entanglement [13,14], since it scales like a bilinear function of the wave function coefficients, the lowest even integer number which is represented by the concurrence. It hence scales like a probability. Besides these physically motivated reasons, there is also a practical one: it is even easier to obtain the convex roof.

### B. States derived from $\Psi_4^4$

The state taken from Eq. (4) is detected by some of the three (4,0) invariants which are called  $C_{ij}^{(4)}$  in Ref. [10], respectively,  $\mathcal{B}_{[4]}^I$ ,  $\mathcal{B}_{[4]}^{II}$ , and  $\mathcal{B}_{[4]}^{III}$  in Ref. [15]. It is a state which has length 4 and hence cannot be detected by the (6,0) filter invariant as the original state considered previously. Due to the symmetries of the state with respect to permutations of the qubits there are only four distinct states in the SL null cone: three states have a (3,1) invariant, and the one with a (2,2) invariant of SU is a bipartite state and therefore is not considered. The three states with (3,1) symmetry are

$$|\Psi_{4;1}^4\rangle = \frac{1}{2}(|0000\rangle + |1100\rangle + |0010\rangle + |0001\rangle), \quad (13)$$

$$|\Psi_{4;2}^4\rangle = \frac{1}{2}(|1111\rangle + |0011\rangle + |0010\rangle + |0001\rangle), \quad (14)$$

$$|\Psi_{4;4}^4\rangle = \frac{1}{2}(|1111\rangle + |1100\rangle + |0010\rangle + |1110\rangle). \quad (15)$$

The notation is the same as in the previous section; it is reflecting where the partial spin flip is acting on.

## III. CONVEX-ROOF CONSTRUCTION

Since we intend to find a state with three-tangles distributed all over the chain and ideally without any concurrences, we first look at the reduced three-site density matrices.

For completeness we give explicit formulas for the line connecting the pure state  $|Z_1\rangle\langle Z_1|$  at  $z_1 = 2p_1 - 1$  with the density matrix

$$\rho = p|\psi_1\rangle\langle\psi_1| + (1-p)|\psi_2\rangle\langle\psi_2|. \quad (16)$$

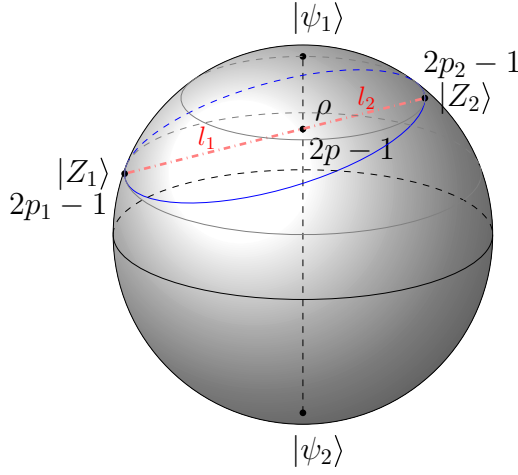


FIG. 1. The Bloch sphere of density matrices made of the orthonormal states  $|\psi_i\rangle$ ,  $i \in \{1, 2\}$ , is shown, together with two superpositions  $|Z_i\rangle$ ,  $i \in \{1, 2\}$ , of them. These two states give a valid decomposition of the density matrix  $\rho$ .

It hits the pure state  $|Z_2\rangle\langle Z_2|$  at  $z_2 = 2p_2 - 1$  on the surface of the Bloch sphere (see Fig. 1). The result is given according to

$$l_1(p_1, p) = \sqrt{1 + (2p - 1)^2 - 2(2p - 1)(2p_1 - 1)}, \quad (17)$$

$$l_2(p_1, p) = \frac{2\sqrt{2}p(1-p)}{\sqrt{1 - 2p(1-p) - (2p-1)(2p_1-1)}}, \quad (18)$$

$$p_2(p_1, p) = \frac{p^2(1-p_1)}{p(p-p_1) + p_1(1-p)}. \quad (19)$$

The lengths  $l_i$ ,  $i \in \{1, 2\}$ , therefore yield the corresponding weights

$$q_1(p_1, p) = \frac{l_2(p_1, p)}{l_1(p_1, p) + l_2(p_1, p)}, \quad (20)$$

$$q_2(p_1, p) = \frac{l_1(p_1, p)}{l_1(p_1, p) + l_2(p_1, p)}, \quad (21)$$

which convexly combine the states  $|Z_i\rangle\langle Z_i|$ ,  $i \in \{1, 2\}$ , to finally decompose  $\rho$  (see Fig. 1).

### A. States derived from $\Psi_6^4$

As already mentioned, the state  $|\Psi_{6,1}^4\rangle$  possesses merely concurrence and no three-tangle. It is therefore similar to the  $W$  states. These states do occur for each number of qubits. We term all those states to be of the  $W$  type, in this case of four qubits, and do not discuss these states any further.

We have two states remaining: (i)  $|\Psi_{6,2}^4\rangle$  and (ii)  $|\Psi_{6,23}^4\rangle$ .

#### 1. The state $|\Psi_{6,2}^4\rangle$

There are only two essentially different cases due to the form invariance of

$$|\Psi_{6,2}^4\rangle = \sqrt{p_1}|1111\rangle + \sqrt{p_2}e^{i\eta}|0111\rangle + c_3|0100\rangle + c_4|0010\rangle + c_5|0001\rangle \quad (22)$$

with respect to permutations of the last three qubits. The state is normalized:  $c_i \in \mathbb{C}$ ,  $i = 2, \dots, 5$ , and  $|c_i|^2 = p_i$ , with  $\sum_{i=1}^5 p_i = 1$ . This leads to two different classes of reduced three-site density matrices to be considered:

$$\begin{aligned} \text{tr}_1 |\Psi_{6,2}^4\rangle\langle\Psi_{6,2}^4| &= p_1|111\rangle\langle 111| + (\sqrt{p_2}e^{i\eta}|111\rangle \\ &+ c_3|100\rangle + c_4|010\rangle + c_5|001\rangle)(\text{H.c.}) \end{aligned} \quad (23)$$

$$\begin{aligned} \text{tr}_2 |\Psi_{6,2}^4\rangle\langle\Psi_{6,2}^4| &= (\sqrt{p_1}|111\rangle + \sqrt{p_2}e^{i\eta}|011\rangle + c_3|000\rangle)(\text{H.c.}) \\ &+ (c_4|010\rangle + c_5|001\rangle)(\text{H.c.}), \end{aligned} \quad (24)$$

with H.c. indicating the Hermitian conjugation. Whereas in the second case both states are already orthogonal, we have to do a bit of algebra in order to construct the eigenstates for the first instance.

By applying a proper local unitary,

$$U = \begin{pmatrix} \cos \alpha & e^{i\chi} \sin \alpha \\ -e^{-i\chi} \sin \alpha & \cos \alpha \end{pmatrix}, \quad (25)$$

with the angle  $\alpha$  and the phase  $\chi$  on the first site, we can diagonalize the matrix  $\text{tr}_1 |\Psi_{6,2}^4\rangle\langle\Psi_{6,2}^4|$ . The conditions for  $\alpha$  and  $\chi$  which derive from the orthogonality relation of the two eigenstates are

$$\tan 2\alpha = \frac{2\sqrt{p_1 p_2}}{1 - 2p_1}, \quad (26)$$

$$\chi = \eta. \quad (27)$$

The corresponding eigenstates of the reduced density matrix are

$$|\psi_1\rangle = (\sin \alpha \sqrt{p_1} + \cos \alpha \sqrt{p_2})e^{i\eta}|111\rangle + \cos \alpha |W_3(0, c_3, c_4, c_5)\rangle, \quad (28)$$

$$|\psi_2\rangle = (\cos \alpha \sqrt{p_1} - \sin \alpha \sqrt{p_2})e^{i\eta}|111\rangle - \sin \alpha |W_3(0, c_3, c_4, c_5)\rangle. \quad (29)$$

These states are normalized to the relative probability with which they occur in the density matrix; hence

$$\rho_1 = \text{tr}_1 |\Psi_{6,2}^4\rangle\langle\Psi_{6,2}^4| = |\psi_1\rangle\langle\psi_1| + |\psi_2\rangle\langle\psi_2|. \quad (30)$$

The corresponding probabilities are the modulus squared of the wave functions, i.e.,

$$P_1 = -p_1 \cos 2\alpha + \sqrt{p_1 p_2} \sin 2\alpha + \cos^2 \alpha, \quad (31)$$

$$P_2 = p_1 \cos 2\alpha - \sqrt{p_1 p_2} \sin 2\alpha + \sin^2 \alpha. \quad (32)$$

Defining  $p_{\text{rel}} = p_1 + p_2$  as the relevant probability for creating a three-tangle in the reduced state, we can parametrize the respective probabilities by  $p_1 = p_{\text{rel}} \cos^2 \beta =: p_{\text{rel}} c$  and  $p_2 = p_{\text{rel}} \sin^2 \beta = p_{\text{rel}}(1 - c)$ , where  $\beta \in [0, \pi/2]$ . Inserting the conditions taken from Eq. (26) leads to

$$P_1 = \frac{1}{2} + \text{sign}(1 - 2p_1) \frac{p_{\text{rel}} c (p_{\text{rel}} c - 2) + p_{\text{rel}}^2 c + \frac{1}{2}}{\sqrt{1 - 4p_{\text{rel}} c + p_{\text{rel}}^2 c (3c + 1)}}. \quad (33)$$

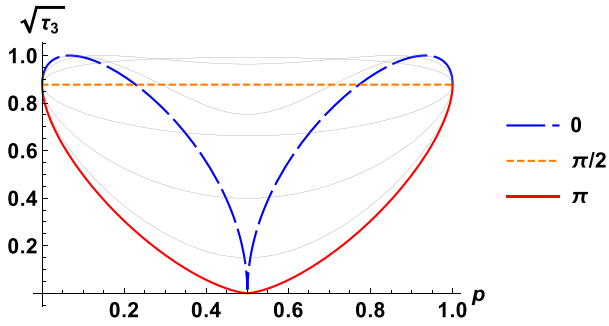


FIG. 2. Characteristic curves for certain values of  $\varphi$ :  $\varphi = 0$  [blue widely dashed curve that interconnects concavely the points at  $p = 0$  and 1 with  $(p, \sqrt{\tau_3}) = (1/2, 0)$ ] to the straight orange dashed line at  $\varphi = \pi/2$  up to  $\varphi = \pi$  (the lowest red curve). The curves are symmetrically distributed around  $\varphi = 0$  and  $\varphi = \pi$ . The red lowest curve is the minimal characteristic curve and is already convex. Therefore it constitutes a lower bound to  $\widehat{\sqrt{\tau_3}}$ . The zero polytope consists of a threefold degenerate zero at the angle  $\varphi = \pi$  and a single zero at  $\varphi = 0$ .

In what follows, we discuss the entanglement in the mixed state

$$\rho_1(p_{\text{rel}}, p) = \frac{p}{P_1} |\psi_1\rangle\langle\psi_1| + \frac{1-p}{1-P_1} |\psi_2\rangle\langle\psi_2|. \quad (34)$$

The pure states under consideration are hence

$$|\Psi(p, \varphi)\rangle := \sqrt{\frac{p}{P_1}} |\psi_1\rangle - e^{i\varphi} \sqrt{\frac{1-p}{1-P_1}} |\psi_2\rangle, \quad (35)$$

and defining  $z = \sqrt{\frac{1-p}{p}} e^{i\varphi}$  (see, e.g., Ref. [16]) we find

$$|\Psi(z)\rangle := \sqrt{\frac{1}{1+|z|^2}} \left( \sqrt{\frac{1}{P_1}} |\psi_1\rangle - z \sqrt{\frac{1}{1-P_1}} |\psi_2\rangle \right), \quad (36)$$

Their three-tangle can be readily read off Eq. (12):

$$\begin{aligned} \tau_3[\Psi(z)] &= 16 \left| \frac{\sin(\alpha + \beta)}{\sqrt{P_1}} - z \frac{\cos(\alpha + \beta)}{\sqrt{1-P_1}} \right| \\ &\times \left| \frac{\cos \alpha}{\sqrt{P_1}} + z \frac{\sin \alpha}{\sqrt{1-P_1}} \right|^3 \frac{\sqrt{p_{\text{rel}}}}{(1+|z|^2)^2} \sqrt{p_3 p_4 p_5}. \end{aligned} \quad (37)$$

This leads to the following two solutions:  $z_{0;1} = \sqrt{\frac{1-P_1}{P_1}} \tan(\alpha + \beta)$  and the threefold  $z_{0;2} = -\sqrt{\frac{1-P_1}{P_1}} \cot \alpha$ , with respective values for  $p_{0;1} = P_1/[P_1 + P_2 \tan^2(\alpha + \beta)]$  and  $p_{0;2} = P_1/(P_1 + P_2 \cot^2 \alpha)$ .

In what follows, we only consider in detail the case  $p_3 = p_4 = p_5 = 1/6$ . We obtain for the angle in this specific instance  $\alpha = \arctan[\sqrt{2}]/2 \approx 0.47766$ . The state  $\Psi_{6;2}^4$  corresponds to  $p_1 = 1/3$ ,  $p_2 = 1/6$ , and  $\eta = 0$ , and appears at the value  $p = (3 + \sqrt{3})/6$  in Fig. 3 [see Eq. (31)]. The characteristic curves, hence the values of  $\sqrt{\tau_3}$ , are shown in Fig. 2 for various values of  $\varphi$ . We refer to Ref. [17] in order to elucidate the procedure.

Valid decompositions of the density matrix, i.e., upper bounds to the convex roof  $\widehat{\sqrt{\tau_3}}$  of  $\sqrt{\tau_3}$  are visualized in Fig. 3. They show various convex combinations of  $\rho$ . The orange

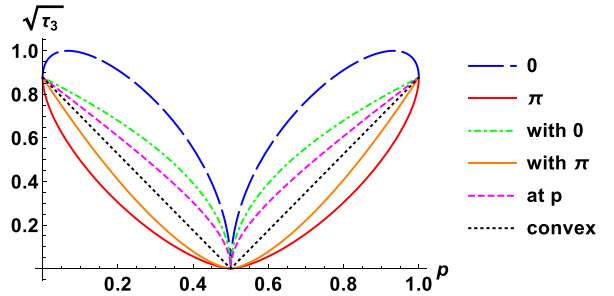


FIG. 3. Upper bounds to the convex roof  $\widehat{\sqrt{\tau_3}}$  of  $\sqrt{\tau_3}$ . The characteristic curves at the angles  $\varphi = 0$  (upper blue widely dashed curve) and  $\varphi = \pi$  (lowest red curve) are shown together with valid decompositions of the density matrix, namely a convex combination of (a) one of the two eigenstates and  $\rho_0 = \frac{1}{2}(|\Psi(\frac{1}{2}, 0)\rangle\langle\Psi(\frac{1}{2}, 0)| + |\Psi(\frac{1}{2}, \pi)\rangle\langle\Psi(\frac{1}{2}, \pi)|)$  (black dotted lines) being a convex sum of states from the zero polytope  $\Psi(\frac{1}{2}, 0)$  and  $\Psi(\frac{1}{2}, \pi)$ , (b)  $|\Psi(p, 0)\rangle\langle\Psi(p, 0)|$  and  $|\Psi(p, \pi)\rangle\langle\Psi(p, \pi)|$  (magenta dashed line), (c) the state  $|\Psi(\frac{1}{2}, 0)\rangle\langle\Psi(\frac{1}{2}, 0)|$  from the zero polytope and the state  $|\Psi(p_2(1/2, p), \pi)\rangle\langle\Psi(p_2(1/2, p), \pi)|$  such that the line connecting both states intersects the center line of the Bloch sphere at  $(2p-1)$  (orange curve below the dotted line) as shown in Fig. 1, and (d) the same as in case (c) but with  $|\Psi(\frac{1}{2}, \pi)\rangle\langle\Psi(\frac{1}{2}, \pi)|$  from the zero polytope and the corresponding state  $|\Psi(p_2(1/2, p), 0)\rangle\langle\Psi(p_2(1/2, p), 0)|$  (green dash-dotted curve above the dashed and dotted line). The orange curve coincides with the convex roof.

curve is given by the expression

$$\widehat{\sqrt{\tau_3}} \left[ \rho_1 \left( \frac{1}{2}, p \right) \right] = \frac{2}{3^{3/4}} |2p-1|^{3/2}; \quad (38)$$

it coincides with the convex roof which we explain in what follows. For  $p_0 = (3 \pm \sqrt{3})/6$  the convex roof of  $\rho_0 := \rho_1(1/2, p_0)$  is  $\widehat{\sqrt{\tau_3}}[\rho_0] = 2/(3\sqrt{3}) \approx 0.3849$ .

As seen in Fig. 2, the characteristic curves are strictly concave around the single zero at  $\varphi = 0$  and  $p = 1/2$ . This has two effects: (i) any deviation around this point of the zero polytope leads to a positive value of the entanglement that is scaling like a square root, and (ii) the weight of the state is furthermore enhanced if more than one state makes up the decomposition, yielding therefore a mixed state. This is equivalent to a seesaw in balance: when one of the parts is moving inwards, it has to become heavier to keep the balance. For these two reasons one of the decomposition states is known to coincide with the pure state corresponding to the single zero of the zero polytope with concave behavior (linear behavior is included). One valid decomposition made of this decomposition state leads to the orange curve in Fig. 3. This acquires the absolute minimum because the characteristic curve at angle  $\varphi = \pi$  is the minimal characteristic curve which in addition is convex. In general one would have to consider also its convexification (see example ahead), but here it is already convex. Thus, any decomposition of pure states gives a resulting three-tangle which lies above that curve, similar to the argument in Ref. [18].

More generally this is true for any rank-two problem of a homogeneous polynomial SL-invariant measure of entanglement of degree  $2m$ , if there exist states which correspond to

an  $n_i$ -fold ( $n_i < m$ ) degenerate solution in the zero polytope that can be combined with the minimal characteristic curve departing from an  $N$ -fold ( $N > m$ ) degenerate solution in the zero polytope to give a decomposition of  $\rho$ , as is the case here. The corresponding minimal characteristic curve can be convexified. This will lead to a lower value for the effective entanglement [19] if the relative gain in entanglement is larger than the relative gain of the weight of the mixed state leading to this convexification. It is *a priori* unclear to us whether this may lead to an entanglement reduction. We can just state that in those cases we have considered here, this was not the case.

If more than one such state exists, then for a given density matrix  $\rho$  the interconnecting straight lines with the minimal characteristic curve will hit the surface of the zero polytope somewhere and we will obtain a curve for the effective entanglement that later has to be convexified to give the convex roof; if it does not intersect the zero polytope, then we obtain a nontrivial lower bound. Due to convexity, it is enough to minimize along the curve on the surface of the

zero polytope that is facing the minimal characteristic curve on the Bloch sphere. We want to mention that here a decrease in the effective entanglement is achieved if mixed states from the surface of the zero polytope are considered. This is due to their relatively higher weight following the seesaw argument given above. A minimization procedure over the finitely many thus-obtained effective entanglement curves will give, after convexification, the convex roof.

For all the states that we consider here, there are two real solutions  $z_{0,i}$  of opposite signs; hence they satisfy the conditions in the former paragraph. Thus, their convex roof is

$$\widehat{\sqrt{\tau_3}}_{\text{est}}[\rho(p)] = q_2(p, p_{0;1})\sqrt{\tau_3[\Psi(p_2(p, p_{0;1}), \pi)]}. \quad (39)$$

For the state

$$\rho_1(p) = \frac{p}{P_1}|\psi_1\rangle\langle\psi_1| + \frac{1-p}{1-P_1}|\psi_2\rangle\langle\psi_2|, \quad (40)$$

we obtain

$$\widehat{\sqrt{\tau_3}}_{\text{est}}[\rho_1(p)] = C(p, p_{0;1})\sqrt{\left|\frac{\sin(\alpha + \beta)}{\sqrt{P_1}} + \sqrt{\frac{1-p_2(p, p_{0;1})}{p_2(p, p_{0;1})}}\frac{\cos(\alpha + \beta)}{\sqrt{1-P_1}}\right|\left|\frac{\cos\alpha}{\sqrt{P_1}} - \sqrt{\frac{1-p_2(p, p_{0;1})}{p_2(p, p_{0;1})}}\frac{\sin\alpha}{\sqrt{1-P_1}}\right|^3}, \quad (41)$$

with  $C(p, p_{0;1}) = 4q_2(p, p_{0;1})p_2(p, p_{0;1})\sqrt[3]{p_{\text{rel}}p_3p_4p_5}$ . In order to give a nonsymmetric example we chose the state corresponding to  $p_1 = 5/9$  and  $p_i = 1/9$  for  $i = 2, \dots, 5$  in Eq. (23); the results are shown in Fig. 4. It can be seen that the relatively minimal characteristic curve corresponding to the threefold solution of the zero polytope is not convex; its convexification is seen as a red dotted curve adapted to the red dashed curve corresponding to the angle  $\pi$  in the plot.

We emphasize here that also one of the upper bounds in Ref. [20] was similar to this type except that the resulting curve was not convex; one should of course consider its convexification for reaching the convex roof. This should be reconsidered in the future.

If the zeros in the zero polytope are not precisely at opposite angles of the sphere, the optimal decomposition in the convex roof will change continuously from this absolutely optimal decomposition that we have in this case. It can therefore be considered as a lower bound for this type of solution and gives a better lower bound than the minimal characteristic curve as used in Refs. [21–24] to lower bound the convex roof making use of the symmetry in certain states.

We briefly come back to the second case, in which the eigenstates can be directly read off Eq. (24). We have

$$\rho_2(\{p_i\}; p) = \frac{p}{P_1}|\psi_1\rangle\langle\psi_1| + \frac{1-p}{P_2}|\psi_2\rangle\langle\psi_2|, \quad (42)$$

where

$$|\psi_1\rangle = \sqrt{p_1}|111\rangle + \sqrt{p_2}e^{i\eta}|011\rangle + c_3|000\rangle, \quad (43)$$

$$|\psi_2\rangle = c_4|010\rangle + c_5|001\rangle, \quad (44)$$

and

$$P_1 = p_1 + p_2 + p_3, \quad (45)$$

$$P_2 = p_4 + p_5. \quad (46)$$

There is only one convex characteristic curve, which is the straight line connecting zero with  $\sqrt{p_1p_3}/(p_1 + p_2 + p_3)$ . Hence

$$\widehat{\sqrt{\tau_3}}[\rho_2(\{p_i\}; p)] = \frac{2p\sqrt{p_1p_3}}{P_1}, \quad (47)$$

which means inserting  $p = P_1$  for  $\rho_2 := \text{tr}_2|\Psi_{6;2}^4\rangle\langle\Psi_{6;2}^4|$ . For the same choice of probabilities as above we get  $\widehat{\sqrt{\tau_3}}[\rho_2] = \frac{\sqrt{2}}{3} \approx 0.4714$ .

At the end, we briefly comment on the CKW inequality noting that for this particular state all concurrences vanish. The extended inequality would however already be satisfied with  $(\widehat{\sqrt{\tau_3}})^2$  as the three-tangle [25–27].

To conclude, we have found four-qubit states with vanishing two- and four-tangles which however possess three-tangles distributed all over the four parties. The states have the form  $|\Psi_{6;2}^4\rangle$  [see Eq. (22)]. They are similar to the  $W$  class which have all of their entanglement stored among two parties distributed all over the chain.

## 2. The state $|\Psi_{6;23}^4\rangle$

The state

$$|\Psi_{6;23}^4\rangle := \sqrt{p_1}|1111\rangle + \sqrt{p_2}e^{i\eta}|0111\rangle + c_3|1011\rangle + c_4|0010\rangle + c_5|0001\rangle,$$

with  $c_i \in \mathbb{C}$ ,  $i = 2, \dots, 5$ ,  $|c_i|^2 = p_i$ , is normalized for  $\sum_{i=1}^5 p_i = 1$ . It is form invariant with respect to permutation of the first qubit and the last two qubits. Hence, there are also two essentially different reduced density matrices to be

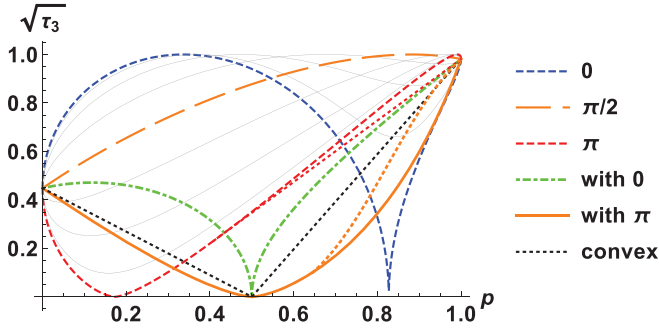


FIG. 4. Some characteristic curves are shown besides those at the angles  $\varphi = 0$  (blue dashed curve that concavely drops to zero at  $p$  about 0.83),  $\varphi = \pi/2$  (orange widely dashed curve), and  $\varphi = \pi$  (red dashed curve that convexly drops to zero at  $p$  about 0.17), together with several valid decompositions of the density matrix and hence upper bounds to the convex roof  $\widehat{\sqrt{\tau_3}}$  of  $\sqrt{\tau_3}$ , namely a convex combination of (a) one of the two eigenstates and  $\rho_0 = \frac{1}{2}(|\Psi(p_{0,1}, 0)\rangle\langle\Psi(p_{0,1}, 0)| + |\Psi(p_{0,2}, \pi)\rangle\langle\Psi(p_{0,2}, \pi)|)$  (black dotted lines) of the states taken from the zero polytope given by  $\Psi(p_{0,1}, 0)$  and a threefold solution in  $\Psi(p_{0,2}, \pi)$ , (b) the state  $|\Psi(p_{0,1}, 0)\rangle\langle\Psi(p_{0,1}, 0)|$  from the zero polytope and a state  $|\Psi(p_2(p_{0,1}, p), \pi)\rangle\langle\Psi(p_2(p_{0,1}, p), \pi)|$  such that the line connecting both states intersects the center line of the Bloch sphere at  $(2p - 1)$  (solid orange curve below the dotted black line), (c) the same as in case (b) but with  $|\Psi(p_{0,2}, \pi)\rangle\langle\Psi(p_{0,2}, \pi)|$  from the zero polytope and the corresponding state  $|\Psi(p_2(p_{0,2}, p), 0)\rangle\langle\Psi(p_2(p_{0,2}, p), 0)|$  (dash-dotted green curve above the dotted black line). The orange curve is already convex and therefore coincides with the convex roof. We also show the convexified characteristic curve (red dotted line attached to the red dashed curve corresponding to the characteristic curve at the angle  $\pi$ ). It however does not lead to a diminishing of the effective three-tangle (dotted orange curve above the convex roof) as one would expect. This is due to the linear increase of weight with decreasing value of  $p$ . It therefore approaches to the convexified characteristic curve for  $p \rightarrow 1$ .

considered. They are

$$\begin{aligned} \text{tr}_1 |\Psi_{6,23}^4\rangle\langle\Psi_{6,23}^4| &= (\sqrt{p_1}|111\rangle + c_3|011\rangle)(\text{H.c.}) \\ &+ (\sqrt{p_2}e^{i\eta}|111\rangle + c_4|010\rangle + c_5|001\rangle)(\text{H.c.}), \end{aligned} \quad (48)$$

$$\begin{aligned} \text{tr}_3 |\Psi_{6,23}^4\rangle\langle\Psi_{6,23}^4| &= p_5|001\rangle\langle 001| + (\sqrt{p_1}|111\rangle \\ &+ \sqrt{p_2}e^{i\eta}|011\rangle + c_3|101\rangle + c_4|000\rangle)(\text{H.c.}). \end{aligned} \quad (49)$$

The first reduced density matrix is written in the subnormalized eigenvector form

$$\rho = |\psi_1\rangle\langle\psi_1| + |\psi_2\rangle\langle\psi_2|, \quad (50)$$

whose subnormalized eigenvectors (obtained with the same method as in the preceding section) are

$$\begin{aligned} |\psi_1\rangle &= (\sqrt{p_1} \cos \alpha - \sqrt{p_2} \sin \alpha)e^{i\eta}|111\rangle \\ &+ c_3e^{i\eta} \cos \alpha|011\rangle - \sin \alpha(c_4|010\rangle + c_5|001\rangle), \end{aligned} \quad (51)$$

$$|\psi_2\rangle = (\sqrt{p_1} \sin \alpha + \sqrt{p_2} \cos \alpha)e^{i\eta}|111\rangle$$

$$+ c_3e^{i\eta} \sin \alpha|011\rangle + \cos \alpha(c_4|010\rangle + c_5|001\rangle), \quad (52)$$

where

$$\tan 2\alpha = \frac{2\sqrt{p_1 p_2}}{1 - 2(p_1 + p_3)}, \quad (53)$$

$$\chi = \eta, \quad (54)$$

and whose three-tangle vanishes.

Only the second reduced density matrix

$$\rho_3 = |\psi_1\rangle\langle\psi_1| + |\psi_2\rangle\langle\psi_2|, \quad (55)$$

with

$$|\psi_1\rangle = \sqrt{p_1}|111\rangle + c_4|000\rangle + \sqrt{p_2}e^{i\eta}|011\rangle + c_3|101\rangle, \quad (56)$$

$$|\psi_2\rangle = \sqrt{p_5}|001\rangle, \quad (57)$$

has a nontrivial three-tangle. Its zero simplex consists of a single point at the end of the interval  $[0,1]$  which goes back to a fourfold-degenerate root. It leads consequently to a single linear characteristic curve. Therefore the convex roof of

$$\rho(\{p_i\}; p) := \frac{p}{1-p_5}|\psi_1\rangle\langle\psi_1| + \frac{1-p}{p_5}|\psi_2\rangle\langle\psi_2| \quad (58)$$

equals

$$\widehat{\sqrt{\tau_3}}[\rho(\{p_i\}; p)] = 2p \frac{\sqrt{p_1 p_4}}{(1-p_5)}, \quad (59)$$

so that we obtain

$$\widehat{\sqrt{\tau_3}}[\rho_3] = 2\sqrt{p_1 p_4}. \quad (60)$$

These states however have always a nonvanishing concurrence  $C[\rho_{ij}] = \sqrt{2p_i p_j}$  and  $\vec{J} = (3, 2, 5, 4)$  for nonvanishing  $p_k$ ,  $k = 2, \dots, 5$ . However, an extended monogamy inequality would be satisfied with  $\widehat{\sqrt{\tau_3}}^2$  as the three-tangle, as before.

## B. States derived from $\Psi_4^4$

As we come to the states derived from  $\Psi_4^4$  there are two cases left to be considered. Inserting arbitrary weights for the state (13) we obtain

$$|\Psi_{4,1}^4\rangle = \sqrt{p_1}|0000\rangle + c_2|1100\rangle + c_3|0010\rangle + \sqrt{p_4}e^{i\eta}|0001\rangle, \quad (61)$$

where the  $c_i$  are complex,  $|c_i|^2 = p_i$ , and which is normalized if  $\sum_{i=1}^4 p_i = 1$ . This state is form invariant under permutations of the first two qubits and the last two qubits, and hence only two different reduced density matrices exist. They consist of two mixed states which have no three-tangled pure state in their range.

The second state has the same form invariance as above. It is

$$|\Psi_{4,2}^4\rangle = c_1|1111\rangle + \sqrt{p_2}|0011\rangle + \sqrt{p_3}e^{i\eta}|0010\rangle + c_4|0001\rangle. \quad (62)$$

So there are only two essentially different reduced density matrices

$$\text{tr}_1 |\Psi_{4,2}^4\rangle\langle\Psi_{4,2}^4| = p_1|111\rangle\langle 111| + (\sqrt{p_2}|011\rangle + \sqrt{p_3}e^{i\eta}|010\rangle + c_4|001\rangle)(\text{H.c.}), \quad (63)$$

$$\text{tr}_4 |\Psi_{4,2}^4\rangle\langle\Psi_{4,2}^4| = p_3|001\rangle\langle 001| + (c_1|111\rangle + \sqrt{p_2}|001\rangle + c_4|000\rangle)(\text{H.c.}). \quad (64)$$

Whereas the first density matrix has no three-tangled state in its range, the eigenstates of  $\text{tr}_4 |\Psi_{4,2}^4\rangle\langle\Psi_{4,2}^4|$  are

$$|\psi_1\rangle \propto \cos\alpha(c_1|111\rangle + c_4|000\rangle) + (\sqrt{p_2}\cos\alpha - \sqrt{p_3}\sin\alpha)|001\rangle, \quad (65)$$

$$|\psi_2\rangle \propto \sin\alpha(c_1|111\rangle + c_4|000\rangle) + (\sqrt{p_2}\sin\alpha + \sqrt{p_3}\cos\alpha)|001\rangle, \quad (66)$$

with the condition for orthogonality of the two vectors being

$$\tan(2\alpha) = \frac{2\sqrt{p_2p_3}}{(2p_3 - 1)}, \quad (67)$$

$$\chi = \eta. \quad (68)$$

The weights of the normalized eigenfunctions are

$$P_1 = \cos^2\alpha - p_3\cos(2\alpha) - \sqrt{p_1p_3}\sin(2\alpha), \quad (69)$$

$$P_2 = \sin^2\alpha + p_3\cos(2\alpha) + \sqrt{p_1p_3}\sin(2\alpha). \quad (70)$$

This state corresponds to a single point in  $\mathbb{C}$  belonging to a fourfold solution for the zero polytope. The convex roof for this situation is known exactly [28]. It is independent of the decomposition of the density matrix; hence it is a linear function connecting the three-tangles of the eigenvectors, which are

$$\sqrt{\tau_3}[\psi_1] = 2\frac{\cos^2(\alpha)\sqrt{p_1p_4}}{P_1}, \quad (71)$$

$$\sqrt{\tau_3}[\psi_2] = 2\frac{\sin^2(\alpha)\sqrt{p_1p_4}}{P_2}. \quad (72)$$

This results in

$$\widehat{\sqrt{\tau_3}}[\text{tr}_4 |\Psi_{4,2}^4\rangle\langle\Psi_{4,2}^4|] = 2\sqrt{p_1p_4}. \quad (73)$$

The remaining state is

$$|\Psi_{4,4}^4\rangle = \sqrt{p_1}|1111\rangle + c_2|1100\rangle + c_3|0010\rangle + \sqrt{p_4}e^{i\eta}|1110\rangle, \quad (74)$$

where  $c_i \in \mathbb{C}$ ,  $|c_i|^2 = p_i$ , and with the same condition  $\sum_{i=1}^4 p_i = 1$  for normalization. This state possesses form invariance with respect to the first two qubits only. The reduced density matrices are

$$\text{tr}_1 |\Psi_{4,4}^4\rangle\langle\Psi_{4,4}^4| = p_2|010\rangle\langle 010| + (\sqrt{p_1}|111\rangle + c_2|100\rangle + \sqrt{p_4}e^{i\eta}|110\rangle)(\text{H.c.}), \quad (75)$$

$$\text{tr}_3 |\Psi_{4,4}^4\rangle\langle\Psi_{4,4}^4| = p_2|010\rangle\langle 010| + (\sqrt{p_1}|111\rangle + c_3|000\rangle + \sqrt{p_4}e^{i\eta}|110\rangle)(\text{H.c.}), \quad (76)$$

$$\text{tr}_4 |\Psi_{4,4}^4\rangle\langle\Psi_{4,4}^4| = p_1|111\rangle\langle 111| + (c_2|110\rangle + c_3|001\rangle + \sqrt{p_4}e^{i\eta}|111\rangle)(\text{H.c.}). \quad (77)$$

The first mixed state has no three-tangled pure state in its whole range; only tracing out the third or the fourth qubit renders a nonzero contribution.

Tracing out the third qubit leads directly to the eigenvectors  $\psi_2 = |010\rangle$  and  $\psi_1 \propto \sqrt{p_1}|111\rangle + c_3|000\rangle + \sqrt{p_4}e^{i\eta}|110\rangle$ , with corresponding eigenvalues  $p_2$  and  $1 - p_2$ , respectively. As above, the convex roof is known exactly to be the linear interpolation between the eigenstates of  $\rho$ , hence between zero and

$$\sqrt{\tau_3}[\psi_1] = \frac{2\sqrt{p_1p_3}}{1 - p_2}. \quad (78)$$

This ultimately gives rise to

$$\widehat{\sqrt{\tau_3}}[\text{tr}_3 |\Psi_{4,4}^4\rangle\langle\Psi_{4,4}^4|] = 2\sqrt{p_1p_3}. \quad (79)$$

Here again, this is trivially seen because the characteristic curves all coincide with a straight line which is hence identical with the already convex lowest characteristic curve. This case also corresponds to a unique fourfold solution of the zero polytope [28].

Tracing out the fourth qubit gives the eigenstates

$$|\psi_1\rangle \propto (\sqrt{p_1}\sin\alpha + \sqrt{p_4}\cos\alpha)|111\rangle + e^{-i\eta}\cos\alpha(c_2|110\rangle + c_3|001\rangle), \quad (80)$$

$$|\psi_2\rangle \propto (\sqrt{p_1}\cos\alpha - \sqrt{p_4}\sin\alpha)|111\rangle - e^{-i\eta}\sin\alpha(c_2|110\rangle + c_3|001\rangle), \quad (81)$$

where

$$\tan(2\alpha) = \frac{2\sqrt{p_1p_4}}{1 - 2p_1}, \quad (82)$$

$$\chi = \eta. \quad (83)$$

The moduli squared of the eigenstates are

$$P_1 = \cos^2\alpha - p_1\cos(2\alpha) + \sin(2\alpha)\sqrt{p_1p_4}, \quad (84)$$

$$P_2 = \sin^2\alpha + p_1\cos(2\alpha) - \sin(2\alpha)\sqrt{p_1p_4}. \quad (85)$$

The convex roof for the three-tangle linearly connects the tangles of the eigenstates [28]

$$\sqrt{\tau_3}[\psi_1] = 2\frac{\cos^2(\alpha)\sqrt{p_2p_3}}{P_1}, \quad (86)$$

$$\sqrt{\tau_3}[\psi_2] = 2\frac{\sin^2(\alpha)\sqrt{p_2p_3}}{P_2}, \quad (87)$$

and hence we have

$$\widehat{\sqrt{\tau_3}}[\text{tr}_4 |\Psi_{4,4}^4\rangle\langle\Psi_{4,4}^4|] = 2\sqrt{p_2p_3}. \quad (88)$$

The only nonzero concurrences are  $C[\rho_{1,2}] = \sqrt{2p_3p_4}$  and  $C[\rho_{3,4}] = \sqrt{2p_1p_2}$ , where  $\rho_{i,j}$  is the reduced density matrix of qubits  $i$  and  $j$ . We state that whenever all the concurrences vanish either all the three-tangles are zero or one is dealing with a bipartite state. We therefore have no perfect analogy to the  $W$  states.

Hence, states derived from  $\Psi_4^4$  never lead to a perfect analog of the  $W$  class.

In all cases the derived states satisfy an extended monogamy relation with  $\sqrt[3]{\tau_3^2}$  inserted as the three-tangle.

#### IV. CONCLUSIONS

In conclusion we have singled out states of four qubits that, differing from the states from the  $W$  class that exclusively contain two-tangles, contain only three-tangles which however are globally distributed. To this end we have analyzed specific four-qubit states which are located in the SL null cone. This guarantees that all possible SL-invariant four-tangles are zero. In order to satisfy this minimal condition, we apply partial spin flips to a  $c$ -balanced state, following Ref. [4]. All states satisfy an extended monogamy relation with  $\sqrt[3]{\tau_3^2}$  inserted as the three-tangle. The possibility to extend the monogamy inequality in that form has however already been excluded [27]. Since the value of the three-tangle will shrink [20] (see also Ref. [29]) with growing  $s$  in  $\sqrt[3]{\tau_3^s}$ , the result will however be upper bounded by its value at  $s = 2$ .

We consider it worth also hinting towards the alternating signs appearing in the monogamy equality of Ref. [30]. It could therefore be that a full analog to the  $W$  state may appear predominantly for an even number of  $n$  of some residual  $n$ -tangle. In order to test this, one should at least analyze corresponding states of five qubits.

Intriguingly, this alternating sum arises in apparently quite various instances: for representations of the universal state inversion [31] and in the shadow inequalities [32,33] from quantum error correction. Here apparently rather different fields such as multipartite entanglement and quantum error correcting codes merge. Also the Gell-Mann representatives for the operator  $\sigma_y$  for qubits emerging from the representation of the general state inversion [31] have also appeared before inside the operator with full SL( $d$ ) symmetry [34] that creates the determinant and is used to form the SL-invariant analog to the concurrence for qubits.

It will be of interest if the various three-tangles can be rendered equal. The latter could be achieved by locally applying SL operations to the states, making use of SL invariants which scale quadratically in  $\psi$  (or linearly in  $\rho$ ) [14,15]. Also it would be intriguing if such states existed for larger numbers of  $Q$  qubits and  $n$ -site entanglement. However, for growing numbers of qubits, the considered reduced density matrices usually are of higher rank and no exact treatment is known so far. An interesting add-on would be whether translationally (or even permutationally) invariant versions of such states exist and whether it is possible to write such a state for an arbitrary number of qubits as for the  $W$  state. It is however clear that the permutationally extended version of the state  $|\Psi_{6;2}^4\rangle$  will always carry a four-tangle except for  $p_2 = 0$  where it becomes a state in the usual  $W$  class.

As an interesting by-product it is demonstrated that the exact convex roof is achieved in the rank-two case of the  $m$ th root of a homogeneous degree  $2m$  polynomial SL-invariant measure of entanglement if there exist states which correspond to a maximally  $m - n$ -fold degenerate solution in the zero polytope that can be combined with the (convexified) minimal characteristic curve of an  $(m + n)$ -fold degenerate solution,  $n \in \mathbf{N}_0$  to give a decomposition of  $\rho$ . The three-tangle has homogeneous degree 4, hence  $m = 2$  for this case. If more than one such state does exist, one has to take the minimum of the results. In case no decomposition of  $\rho$  is reached, the minimum over the thus-constructed states represents a lower bound to the SL-invariant entanglement measure under consideration; it is of course larger than the lowest characteristic curve employed in Refs. [22] for quantifying the three-tangle of the GHZ-Werner state [21] which has then been applied further [35,36].

#### ACKNOWLEDGMENTS

We acknowledge fruitful discussions with R. Schützhold and F. Huber. This work was supported by SFB 1242 of the German Research Foundation (DFG).

- 
- [1] V. Coffman, J. Kundu, and W. K. Wootters, *Phys. Rev. A* **61**, 052306 (2000).
  - [2] T. J. Osborne and F. Verstraete, *Phys. Rev. Lett.* **96**, 220503 (2006).
  - [3] W. Dür, G. Vidal, and J. I. Cirac, *Phys. Rev. A* **62**, 062314 (2000).
  - [4] M. Johansson, M. Ericsson, E. Sjöqvist, and A. Osterloh, *Phys. Rev. A* **89**, 012320 (2014).
  - [5] A. Osterloh and J. Siewert, *Int. J. Quantum Inf.* **4**, 531 (2006).
  - [6] A. Osterloh and J. Siewert, *New J. Phys.* **12**, 075025 (2010).
  - [7] J.-G. Luque, J.-Y. Thibon, and F. Toumazet, *Math. Struct. Comput. Sci.* **17**, 1133 (2007).
  - [8] M. Johansson, M. Ericsson, K. Singh, E. Sjöqvist, and M. S. Williamson, *Phys. Rev. A* **85**, 032112 (2012).
  - [9] A. Osterloh and J. Siewert, *Phys. Rev. A* **72**, 012337 (2005).
  - [10] D. Ž. Đoković and A. Osterloh, *J. Math. Phys.* **50**, 033509 (2009).
  - [11] A. Wong and N. Christensen, *Phys. Rev. A* **63**, 044301 (2001).
  - [12] F. Verstraete, J. Dehaene, and B. De Moor, *Phys. Rev. A* **68**, 012103 (2003).
  - [13] F. Verstraete, J. Dehaene, B. De Moor, and H. Verschelde, *Phys. Rev. A* **65**, 052112 (2002).
  - [14] O. Viehmann, C. Eltschka, and J. Siewert, *Appl. Phys. B* **106**, 533 (2012).
  - [15] O. Viehmann, C. Eltschka, and J. Siewert, *Phys. Rev. A* **83**, 052330 (2011).
  - [16] A. Osterloh, J. Siewert, and A. Uhlmann, *Phys. Rev. A* **77**, 032310 (2008).
  - [17] A. Osterloh, *Phys. Rev. A* **94**, 062333 (2016).
  - [18] R. Lohmayer, A. Osterloh, J. Siewert, and A. Uhlmann, *Phys. Rev. Lett.* **97**, 260502 (2006).
  - [19] We use the name *effective entanglement* since it emerges from a real decomposition of a given density matrix. It therefore is a reasonable upper bound to the convex roof which could effectively be the entanglement of that particular state.
  - [20] A. Osterloh, *Phys. Rev. A* **94**, 012323 (2016).

- [21] C. Eltschka and J. Siewert, *Phys. Rev. Lett.* **108**, 020502 (2012).
- [22] J. Siewert and C. Eltschka, *Phys. Rev. Lett.* **108**, 230502 (2012).
- [23] C. Eltschka and J. Siewert, *Phys. Rev. A* **89**, 022312 (2014).
- [24] G. Sentís, C. Eltschka, and J. Siewert, *Phys. Rev. A* **94**, 020302(R) (2016).
- [25] B. Regula, S. Di Martino, S. Lee, and G. Adesso, *Phys. Rev. Lett.* **113**, 110501 (2014).
- [26] B. Regula, S. Di Martino, S. Lee, and G. Adesso, *Phys. Rev. Lett.* **116**, 049902(E) (2016).
- [27] B. Regula, A. Osterloh, and G. Adesso, *Phys. Rev. A* **93**, 052338 (2016).
- [28] B. Regula and G. Adesso, *Phys. Rev. Lett.* **116**, 070504 (2016).
- [29] C. Eltschka, A. Osterloh, and J. Siewert, *Phys. Rev. A* **80**, 032313 (2009).
- [30] C. Eltschka and J. Siewert, *Phys. Rev. Lett.* **114**, 140402 (2015).
- [31] C. Eltschka and J. Siewert, *Quantum* **2**, 64 (2018).
- [32] F. Huber, C. Eltschka, J. Siewert, and O. Gühne, *J. Phys. A* **51**, 175301 (2018).
- [33] E. M. Rains, *IEEE Trans. Inf. Theory* **46**, 54 (2000).
- [34] A. Osterloh, *J. Phys. A* **48**, 065303 (2015).
- [35] C. Eltschka and J. Siewert, *Sci. Rep.* **2**, 942 (2012).
- [36] C. Eltschka and J. Siewert, *Quantum Inf. Comput.* **13**, 210 (2013).